Free-Breathing, Self-Navigated and Dynamic 3-D Multi-Contrast Cardiac CINE Imaging Using Cartesian Sampling and Compressed Sensing

Elisabeth Hoppe[1], Jens Wetzl[2], Christoph Forman[2], Gregor Körzdörfer[2,3], Manuel Schneider[1], Peter Speier[2], Michaela Schmidt[2], and Andreas Maier[1]

[1]Pattern Recognition Lab, Friedrich-Alexander-Universität Erlangen-Nürnberg, Erlangen, Germany, [2]Magnetic Resonance, Siemens Healthcare GmbH, Erlangen, Germany, [3]Friedrich-Alexander-Universität Erlangen-Nürnberg, Erlangen, Germany

Synopsis

We present a free-breathing multi-contrast 3-D cardiac CINE acquisition and reconstruction technique based on Compressed Sensing. Inversion pulses were repeatedly applied during a continuous acquisition to sample contrast- and cardiac-resolved 3-D data, while a self-navigation method was applied for respiratory gating. Validation was performed in a phantom, showing recovery curves and T_1* maps in good correlation to known T_1 values for the phantom as well as a MOLLI reference measurement. Feasibility for in-vivo application was demonstrated in a healthy volunteer.

Introduction

Cardiac CINE imaging provides anatomical and functional information from one scan. Additionally, with a 3-D sequence, increased SNR, high through-plane resolution and retrospective view reformations are possible. However, this would provide single-contrast images only and thus no additional information like T_1 values can be derived for classifying e.g. diffuse fibrosis [1,2] or edema [3]. We present a multi-contrast cardiac CINE acquisition and reconstruction technique based on 3-D CINE and Compressed Sensing [4,5] to address this limitation. Our 3-D high-resolution, dynamic scan during free-breathing offers the possibility of acquiring contrast- and cardiac-resolved data from one acquisition. This can be used for a retrospective analysis of the data and the derivation of other characteristics as T_1 relaxation.

Methods

Sequence

We acquired data during free-breathing using a 3-D volume-selective, ECG-gated, prototype balanced Steady-State-Free-Precession (bSSFP) sequence. Adiabatic inversion (IR) pulses were applied every $3s$ to sample multi-contrast CINE (MC-CINE) data. Waiting periods of variable length x were placed after each $3s$ while maintaining the steady state to avoid coherence between the IR pulse and the R wave (Fig.1A). Incoherent subsampling of the Cartesian phase-encoding plane was achieved with a spiral spokes sampling pattern [4]. The first sample of each spiral arm in the k-space center was utilized to derive the respiration signal for respiratory gating.

Retrospective binning and reconstruction

Acquired readouts were sorted into a multi-dimensional space according to their positions after the R wave and the IR pulse (Fig.1B). Afterwards, data was binned into m cardiac and n contrast phases. Prototype image reconstruction was performed separately for every contrast phase, but jointly for all readouts using a previously published Compressed Sensing approach [4,5], resulting in one 3-D volume for every cardiac and contrast phase.

Experiments

All experiments were performed on a 1.5T scanner (MAGNETOM Aera, Siemens Healthcare, Erlangen, Germany). For validation of our method, we acquired undersampled MC-CINE data of the T_1 array of the NIST/ISMRM phantom [6] with a simulated heart rate of 60 beats per minute. Afterwards, data was binned (m=10 cardiac, n=20 contrast phases) resulting in 200 3-D datasets. To show the resulting range of reconstructed contrasts, we fit apparent T_1^* values using the three-parameter fit [7,8]. For comparison, we acquired slices of the phantom from the same position as for the MC-CINE acquisition with a state-of-the-art MOLLI [8] protocol provided by the scanner manufacturer. T_1^* values from our method were obtained from the mean of 5 reconstructed slices, corresponding to one 8 mm thick MOLLI slice at this position. Regions-of-interest (ROIs) within 10 spheres (range: 90 to 2050 ms, representing physically relevant T_1 values within the heart) were segmented manually, and the mean and standard deviations within the ROIs were computed, respectively. Feasibility in a healthy volunteer (m, 20 years) was studied by performing a scan in short-axis (SA) orientation. Data was binned (m=10 cardiac, n=20 contrast phases) and reconstructed. Detailed acquisition and reconstruction parameters are provided in Table 1.

Results

Quantitative T_1* values within the phantom show agreement with MOLLI and ground truth values, with a slight underestimation, but with reduced standard deviations within the ROIs (Fig.2). Results for one volunteer are shown in Fig.3 (respiration detection and gating) and in Fig.4 (reconstructed and reformatted data).

Discussion

Compressed Sensing enables reconstruction of highly undersampled data due to the accelerated acquisition and the binning process. Quantitative comparison of our method with state-of-the-art MOLLI mapping [8] was shown by fitting T_1^* values from multi-contrast volumes. The fitted values from our MC-CINE reveal a slight underestimation compared to MOLLI as no correction is applied. The same correction factor as for MOLLI [8] is not applicable for MC-CINE, as inverted magnetization does not relax back to its initial value due to the continuous acquisition without resting periods. However, MC-CINE leads to smaller standard deviations compared to MOLLI due to the higher SNR. For in-vivo data, binning to the same number of contrast and cardiac phases as for phantom data leads to larger acceleration factors, as fewer readouts can be used due to respiratory gating. Nevertheless, the reconstructed data still can resolve the different contrast and cardiac phases allowing arbitrary reformations to different views.

Conclusion

We proposed a 3-D, multi-contrast, cardiac CINE acquisition and reconstruction method based on Cartesian sampling and Compressed Sensing. This offers the possibility to provide anatomical and functional imaging with multiple contrasts from one continuous scan. Accurate fitting of T_1^* values was shown in phantom data, and feasibility was demonstrated in a volunteer scan. Future work will concentrate on T_1 correction for continuous acquisition and in-vivo experiments.

Acknowledgements

No acknowledgement found.

References

[1] Bull, Sacha, et al. "Human non-contrast T1 values and correlation with histology in diffuse fibrosis." Heart (2013): heartjnl-2012.

[2] Sibley, Christopher T., et al. "T1 Mapping in cardiomyopathy at cardiac MR: comparison with endomyocardial biopsy." Radiology265.3 (2012): 724-732.

[3] Ferreira, Vanessa M., et al. "Non-contrast T1-mapping detects acute myocardial edema with high diagnostic accuracy: a comparison to T2-weighted cardiovascular magnetic resonance." Journal of cardiovascular magnetic resonance 14.1 (2012): 42.

[4]Wetzl, Jens, et al. "Free-breathing, self-navigated isotropic 3-D CINE imaging of the whole heart using Cartesian sampling." Proceedings of the 24th Annual Meeting of ISMRM. Vol. 411. 2016.

[5] Liu, J., Rapin, J., Chang, T. C., Lefebvre, A., Zenge, M., Mueller, E., & Nadar, M. S. (2012, May). Dynamic cardiac MRI reconstruction with weighted redundant Haar wavelets. In ISMRM (Vol. 20, p. 178).

[6] High Precision Devices, Inc. Calibrate MRI Scanners with NIST Referenced Quantitative MRI (qMRI) Phantoms (QIBA DWI and ISMRM). http://www.hpd-online.com/MRI-phantoms.php. Accessed October 16, 2017.

[7]Jara, Hernán. Theory of quantitative magnetic resonance imaging. Hackensack, NJ: World Scientific, 2013. ISBN: 978-981-4295-23-9.

[8] Messroghli, Daniel R., et al. "Modified Look-Locker inversion recovery (MOLLI) for high-resolution T1 mapping of the heart." Magnetic Resonance in Medicine: An Official Journal of the International Society for Magnetic Resonance in Medicine 52.1 (2004): 141-146.

Figures

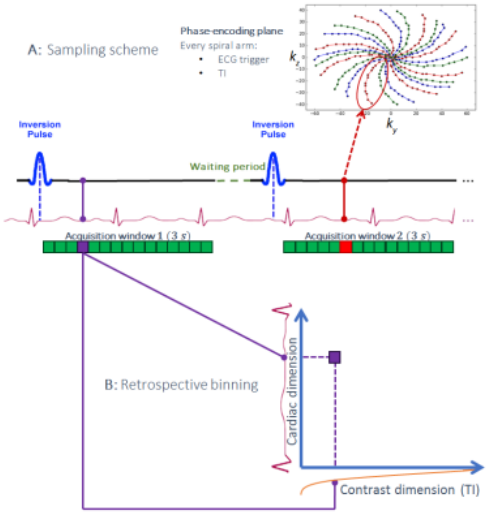

Figure 1: Acquisition scheme. After one IR pulse, continuous readouts are acquired for 3 s over multiple heartbeats. Afterwards, a waiting period is included to vary the position of the IR pulse within the heart cycle.

A: Sampling scheme. Every spiral spoke arm is identified using its position after one R wave and IR pulse (one example is shown in red color, from [7]).

B: Retrospective binning process. One example is shown in purple color: One spiral spokes arm is sorted into the multi-dimensional space according to two dimensions: its position after one R wave (cardiac) and its TI (contrast).

Acquisition	MC-CINE Phantom	MC-CINE In-vivo	MOLLI Phantom
Field-of-view	272×272×60 mm³	340×270×104 mm³	272×272×64 mm³
Resolution	(1.5mm)³	1.9² × 2.0 mm³	1.5²×8.00 mm³
Acquisition duration	6.6 min	6.0 min	2.9 min
TR	2.76 ms	2.49 ms	2.60 ms
TE	1.17 ms	1.06 ms	1.07 ms
α	37°	37°	35°
Acceleration	2.6	2.6	2

Reconstruction	MC-CINE Phantom	MC-CINE In-vivo
Regularization	5^{-3}	$5^{-3} - 10^{-2}$ (dependent on acceleration)
Iterations	40	
Mean acceleration per bin	10.5	15.3
Contrast bins (resolution)	20 (150 ms)	
Cardiac bins (resolution)	10 (100 ms)	10 (75 ms)

Table 1: Acquisition and reconstruction parameters for phantom and in-vivo experiments.

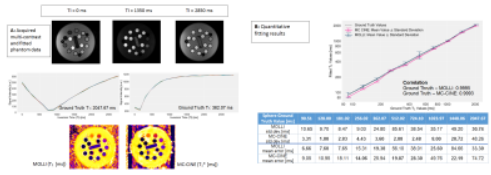

Figure 2: Phantom results.

A: One slice at different TIs (first row) and two recovery curves (each with 10 cardiac phases) of one position within two example spheres (second row) and examples of fitted maps (third row).

B: Comparison of mean values ± standard deviations for ROIs within phantom spheres between MC-CINE (mean values of the 10 cardiac phases for one ROI), MOLLI and ground truth. Note the decreased standard deviations from MC-CINE within the fitted values (table below). From the slight underestimation, the MC-CINE mean error is larger than MOLLI mean error for some cases.

Std.dev.: Standard deviation

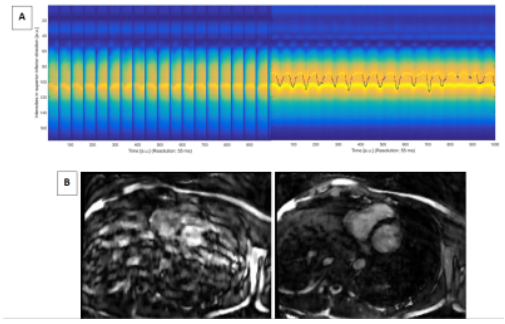

Figure 3: Respiration.

A: Excerpt of central k-space readouts of the volunteer (one coil) used to derive his respiration. Left: Raw signal. Signal gaps resulting from the different contrasts after IR pulses hamper the derivation of the respiration curve. Right: Processed and interpolated signal, from which the respiration curve (blue) is fitted based on SVD. The yellow marked positions on the curve belong to the respiration phase selected for the reconstruction of the data.

B: One example slice reconstructed from all acquired data (left) differ from the same slice reconstructed using our respiration gating method and the same parameters (right).

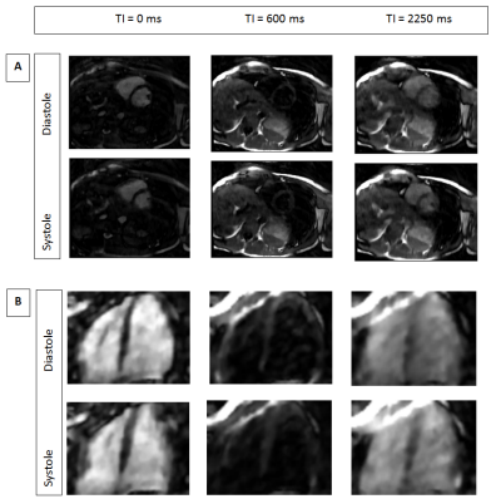

Figure 4: Feasibility results of one volunteer (m, 20 years). Our method can provide different image contrasts for different cardiac phases (A). Every cardiac and contrast phase can be reformatted to a long-axis view (B).